Perpendicular and in-plane magnetic anisotropies in Cr-buffered Fe(x)/MgO interface from first-principles approach

Sci. Rep. Kanazawa Univ.
Vol. 62, pp. 23–35, 2018

ARTICLES

Perpendicular and in-plane magnetic anisotropies in Cr-buffered Fe(x)/MgO interface from first-principles approach

Nurul IKHSAN[1,2]*, Tomosato KANAGAWA[1], Indra PARDEDE[1,3], Daiki YOSHIKAWA[1], and Tatsuki ODA[1,4]

[1]Graduate School of Natural Science and Technology, Kanazawa University, Kanazawa, 920-1192, Japan
[2]School of Computing, Telkom University, Bandung 40257, Indonesia
[3]Department of Physics, Institut Teknologi Sumatera, Lampung 35365, Indonesia
[4]Institute of Science and Engineering, Kanazawa University, Kanazawa, 920-1192, Japan

(Received June 25, 2018 and accepted in revised from August 23, 2018)

Abstract Electronic structure and magnetic anisotropy energy (MAE) of Cr-buffered Fe/MgO interface were investigated in terms of thickness dependence by means of a fully relativistic density functional approach. The electronic structure indicated that the interface state gets occupied unlike a typical rigid band picture as the number of Fe layers decreases, leading large perpendicular anisotropies in the oscillating behavior for its thickness dependence. The maximum of the MAE originating from spin-orbit interaction (SOI) reaches 2mJ/m^2. It was found that the saddle point nature and dispersionless at the Fermi level may be an origin of its large perpendicular magnetic anisotropy. To evaluate the MAE originating from SOI, the in-plane shape magnetic anisotropy originating from magnetic dipole interaction (MDI) was estimated. The calculated MAE from MDI required a suppression of the calculated total magnetization for realizing a fair agreement with an experimental MAE. With using a rescaled magnetization it was found that a possible perpendicular anisotropy may appear in the thickness range of experimental data.

Keywords. magnetic anisotropy, magnetic thin film, Fe/MgO interface, MRAM

1 Introduction

Metal-insulator interface has been attractive in material science for the last decade. The interface of magnetic-oxide, such as Fe/MgO family, holds an important role in the development of magnetoresistive random access memory (MRAM) [1–4]. In the early development stage the modulation of the ferromagnetic free layer is driven by the spin transfer torque mechanism [5, 6]. The challenge is not only the magnetization control, but also large tunnel magnetoresistance [7] and low damping constant [8]. These three are required to realize MRAM applications.

*Corresponding author Email: ikhsan@cphys.s.kanazawa-u.ac.jp

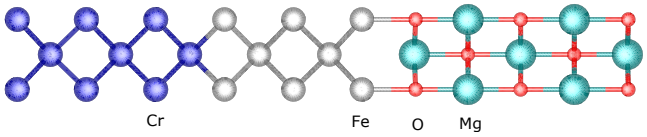

Figure 1: Schematic diagram of the slab systems; Cr(6ML)/Fe(xML)/MgO(5ML) for $x = 5$.

Subsequent advancement of the magnetization control by electric field effect on this interface is discovered [9]. Later, it can be controlled by spin-orbit torque (SOT) [10], and the combination of voltage control and spin-Hall effect of the underlayer, which is also known as voltage-control-spintronics-memory (VoCSM) [11]. Even now the evolution of read-write mechanism still develops, but the fundamental object remains the same Fe/MgO interface. The unique characteristics, like perpendicular magnetic anisotropy (PMA) and spin transfer (voltage, spin torque or VoCSM) controlled magnetic junction, are promising for information technology device, especially for high density and low power consumption data storage [12]. Recently, the unique spin structure with voltage controlled Dzyaloshinskii-Moriya interaction was also discovered in this interface [13]. Such multi-functional interface has a lot of interesting physical properties and potential applications for spintronics or magnonic devices [14].

In the works for the development of the devices, the family of Fe/MgO interfaces has been used as a kernel technological element. They have shown a strong perpendicular magnetic anisotropy for the thin Fe without any heavy element [7, 15]. The multi-functional properties, mentioned in the previous paragraphs, are mostly originated from the electronic structure. In such system, the interface state has been discussed in the several works [16, 17]. These states are consequences of the band formation consisting of non-bonding orbitals on the interface. Although such character has been observed as interesting characteristics, detail dependence of electronic structure has not been investigated.

The recent improvement of computational performance allows us to estimate the magnetic anisotropy or its EF effect precisely and numerically [18–20]. Such improvement contributes not only to physical and qualitative explanations in the property of magnetic anisotropy, but also to semi-quantitative agreements. In particular, the slope in the EF variation has been proved to have a realistic meaning, when compared with the experimental results [21]. On the magnetic anisotropy energy (MAE), the comparison with experiment has a distance from explaining the experimental measurements with a quantitative agreement. The experimental progress on the interface magnetic anisotropy in the thin films gives us a fascinating opportunity on a direct comparison between the theoretical and experimental approaches.

This work was devoted to the discussions on electronic, magnetic, and structural properties of Fe(x ML)/MgO(001), as a reinvestigation in the viewpoint of two dimensional electronic structure. We obtained remarkable Fe-thickness dependences of MAE, implying a picture of non-rigid band filling in the interface states. These results are discussed in terms of electronic band theory, compared with the available experimental data. In the comparison, we also discuss the computational accuracy on MAE within the current state-of-the-art for density functional theory (DFT).

2 Model and method

In order to investigate the interface of Fe/MgO, we consider a slab system, vacuum (0.79 nm)/Cr(w ML)/Fe (x ML)/MgO (5 ML)/vacuum (0.79 nm) (ML=atomic monolayer), in the computation

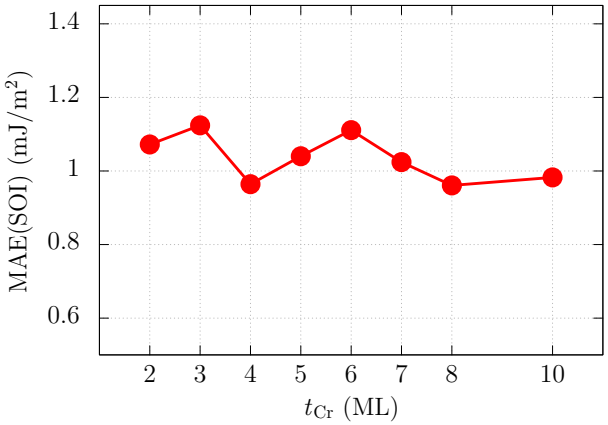

Figure 2: Thickness dependence of Cr layer on MAE in Cr/Fe(3ML)/MgO.

(Fig. 1). The atoms are specified by number as Cr(1), Cr(2), ..., Fe (1), Fe (2), ..., O (1), ..., Mg (1), ... etc. from the Fe/MgO interface. At this interface, an Fe atom was placed just next to the O atom due to its stability, and in the Cr and Fe layers the body-centered layer-stacking sequence was used [22, 23]. The in-plane lattice constant extracted from bulk Cr was employed. The thickness of Fe thin layer (x) was varied from 1 ML to 10 ML.

We carried out first-principles density functional calculations, which employ fully relativistic (with spin-orbit interaction) and scalar-relativistic (without spin-orbit interaction) ultrasoft pseudopotentials and planewave basis [24, 25], by using the generalized gradient approximation [26]. In these calculations, the smearing of Fermi-Dirac function with 315 K was introduced as in the previous works [27, 28]. As the result, the total energy E_{tot}, which has a variational property in the occupation number as well as in the wavefunction and the atomic coordinate. The MAE originating from spin-orbit interaction (SOI) was estimated from the total energy difference between the different magnetization directions [100] (x-axis) and [001] (z-axis), $\mathrm{MAE(SOI)} = E[100] - E[001]$, where [001] specifies the direction of film thickness (right-hand side in Fig. 1). We used the $32 \times 32 \times 1$ mesh of $\mathbf{k}$ point sampling [29] in MAE estimation [30]. Using the scalar-relativistic level computation, in which a $\mathbf{k}$-mesh of $24 \times 24 \times 1$ is used, we induced structural relaxation while keeping both the in-plane lattice constant and the atomic coordinates of O(3). The MAE from the shape anisotropy, MAE(MDI), was estimated using the magnetostatic dipole interaction (MDI) and assuming the atomic magnetic moments obtained by the density functional calculation [31]. In our work, the thickness of Cr layer was set to 6 ML ($w = 6$). Fig. 2 shows the thickness dependence of MAE for the Fe 3ML ($x = 3$) system with the in-plane lattice constant extracted from Fe bcc bulk which is very similar to that of Cr bulk. In Fig. 2 the MAE is almost independent of Cr thickness within the accuracy of 0.1mJ/m^2 for a given Fe thickness. Note that the contribution of Cr surface with vacuum to the MAE(SOI) is negligible. This was confirmed in a free standing Cr layer.

3 Results

3.1 MAE(SOI)

We report the thickness dependence of MAE(SOI) in Fig. 3. It indicates an oscillating perpendicular anisotropy with respect to Fe thickness (x), and the maximum of 2.0 mJ/m^2 at Fe 2ML($x = 2$)

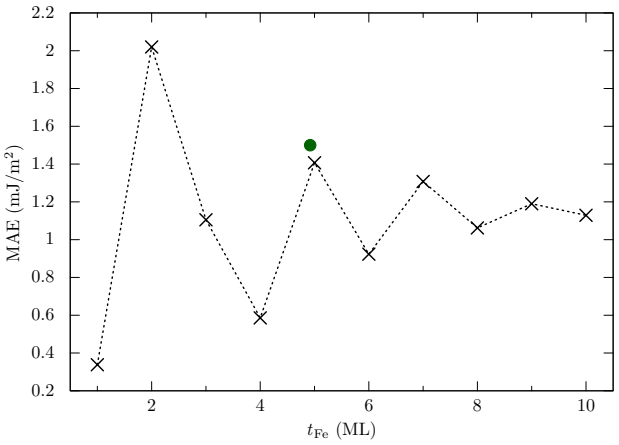

Figure 3: Thickness dependence of the magnetic anisotropy energy (MAE) from spin-orbit interaction in Cr/Fe(xML)/MgO. The bullet indicates the experimental value (ref. [4]), where 1ML thickness is assumed to be 0.142 nm.

and other maximal values at 5ML($x = 5$) and 7ML($x = 7$). The behavior shows that an odd-even alternating oscillation at the thicker systems (4ML-10ML). For the thinner systems, the amplitude of oscillation is largely enhanced since large changes are expected in the electronic structure around the Fe/MgO interface. Hallal et al. also reported an oscillating MAE as a function of Fe thickness [20]. In their system, the thickness varies from 5ML to 13ML in a multi-layer of Fe/MgO with a double interface, while our slab model has the single Fe/MgO interface and more realistic in accordance with the experimental measurement [4].

3.2 Fe 2ML case

The maximum MAE at Fe 2ML is much larger than the previous theoretical and experimental values in the Fe/MgO interface family, comparable to the interface contribution extracted from the extrapolation fitting in the experiment [32]. At Fe 5ML our value agrees well with the experimental value [4].

Figure 4 shows the projected density of states (PDOS) at the interface in $x = 2$ and band dispersions with $3d$ orbital components in the vicinity of the Fermi level (E_{F}). As shown, the E_{F} is located between the two peaks of PDOS consisting of $3d$ orbitals. These electronic states are relatively localized since the main orbital components are made of the non-bonding $3d$-orbitals. Indeed, the states form a flat band around the $\mathbf{k}$-point $\mathbf{k}_1 = \pi/a(1/2, 1/2)$ (see Fig. 4) and a saddle point near $\mathbf{k}_1$ in two-dimensional Brillouin zone (2DBZ). The band flatness appears along $\bar{\mathrm{X}}$–$\bar{\mathrm{Y}}$ line in 2DBZ. These features are remarkably observed for both the occupied and unoccupied bands in Fig. 4(c). There is a saddle point nature around $\mathbf{k}_1$ in 2DBZ (not exact of saddle point). Along $\bar{\mathrm{X}}$–$\bar{\mathrm{Y}}$, there is a maximum at $\mathbf{k}_1$ in the $3d$-orbital band just above E_{F}, and simultaneously along $\bar{\Gamma}$–$\bar{\mathrm{M}}$ a minimum near $\mathbf{k}_1$.

This feature is the origins of sharp PDOS peaks in the interface states, appearing more or less in the Fe/MgO and its family systems. However, for realizing such features, there may be a combination of two conditions. The one is an appropriate orbital hybridization between 1st Fe and 2nd Fe layers. This keeps splitting the mixed eigenstates of d_{xz} and d_{yz} components at $\bar{\mathrm{M}}$ point to the lower and higher eigen energies, while in the Fe 1ML system, those stays remain on or around E_{F} [33]. The 2nd condition is also an orbital hybridization between Fe $d_{3z^2-r^2}$ and O p_z. This keeps

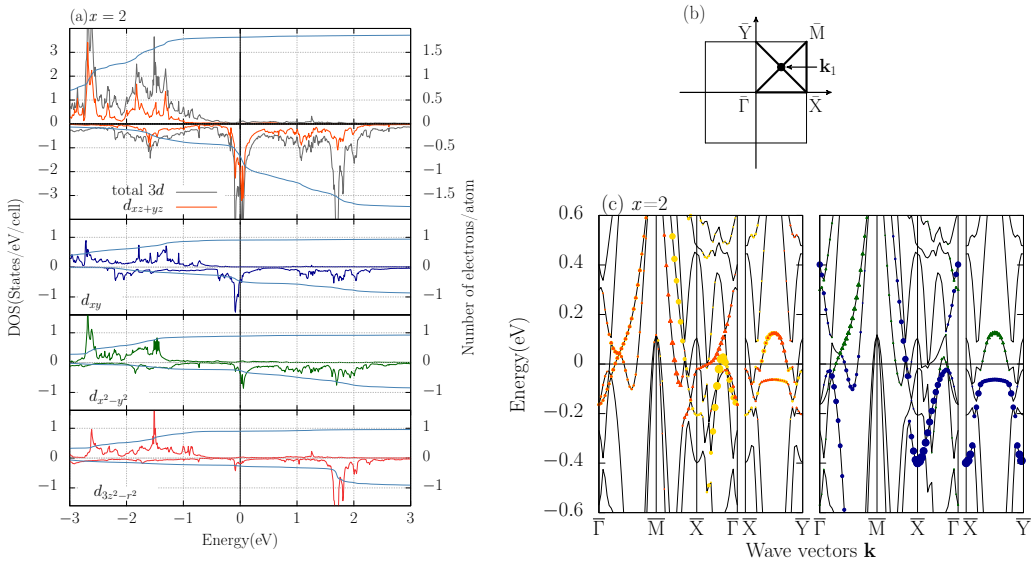

Figure 4: Electronic structures at the Fermi level in Cr/Fe(2ML)/MgO without including spin-orbit interaction, (a) projected densities of states (PDOS)(form the top) 3d total d_{xz+yz}, d_{xy}, $d_{x^2-y^2}$,$d_{3z^2-r^2}$ components, (b) selected **k**-point path, and (c) band dispersion for the Fe 3*d* orbitals at the interface Fe(1). The colors of grey, orange (yellow), blue, green, and red are used for indicating the components of total 3*d* orbital, d_{xz+yz}, d_{xy}, $d_{x^2-y^2}$, and $d_{3z^2-r^2}$, respectively. The light blue curve in (a) indicates integrated number of electrons of each orbital component.

the $d_{3z^2-r^2}$ away from E_F, not disturbing the localized states of non-bonding d_{xy}, $d_{x^2-y^2}$, d_{xz}, and d_{yz} at E_F. The latter has been well known as one of important origins for realizing perpendicular anisotropy [15]. This is because the orbital $d_{3z^2-r^2}$ always contributes only to in-plane magnetic anisotropy, assuming that the contribution from the majority spin state can be neglected due to a large exchange splitting [33]. The MAE maximum in Fe 2ML is obtained as the consequences of the origins discussed above. Note that there are vertical couplings of SOI around $\mathbf{k}_1$ area in 2DBZ, which contribute to perpendicular anisotropy; couplings of d_{xy}–$d_{x^2-y^2}$ and d_{xz}–d_{yz}.

3.3 Fe 5ML case

In $x = 5$, such dispersionless states is more clearly observed just above E_F (0.1 eV in Fig. 5(b)), the band changes upward along $\bar{\Gamma}$–$\bar{M}$ and slightly downward along $\bar{X}$–$\bar{Y}$. In the more real-life scenario of $x = 5$ configuration in Fig. 5, the formation of interface state is also observed, but unfortunately the vertical coupling of d_{xy}–$d_{x^2-y^2}$ and d_{xz}–d_{yz} at $\mathbf{k}_1$ is already shifted away from the Fermi level to higher energy. Therefore we have lower value in the magnetic anisotropy energy, but we still have the coupling of d_{xz}–d_{yz} orbital at middle point of $\bar{X}$–$\bar{\Gamma}$ and $\bar{\Gamma}$–$\bar{M}$ which is contribute significantly to the perpendicular magnetic anisotropy.

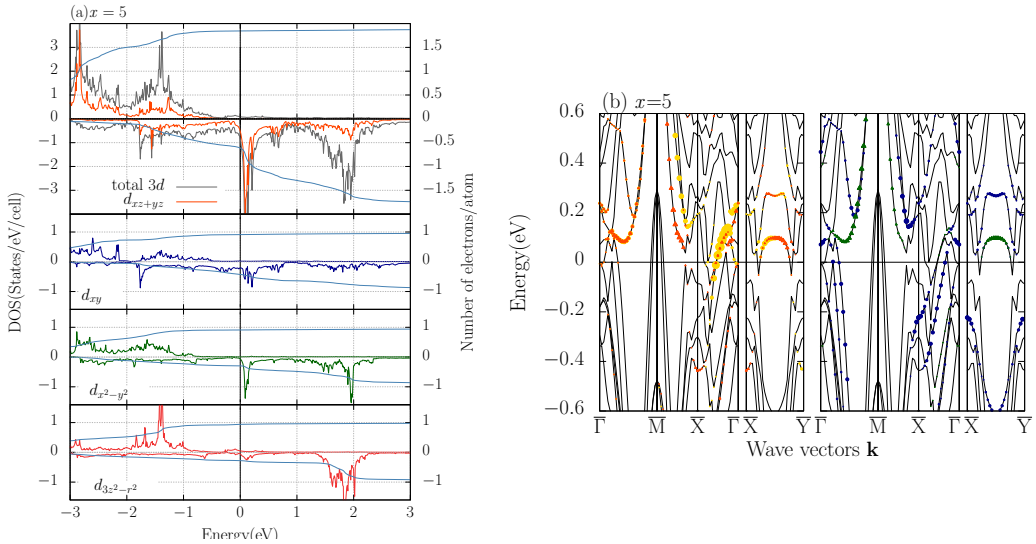

Figure 5: Electronic structures at the Fermi level in Cr/Fe(5ML)/MgO without including spin-orbit interaction, (a) partial density of states (PDOS), (b) band dispersion for the Fe 3d orbitals at the interface Fe(1). The colors of grey, orange (yellow), blue, green, and red are used for indicating the components of total 3d orbital, d_{xz+yz}, d_{xy}, $d_{x^2-y^2}$, and $d_{3z^2-r^2}$, respectively. The light blue line in (a) indicates integrated number of electrons of each orbital component.

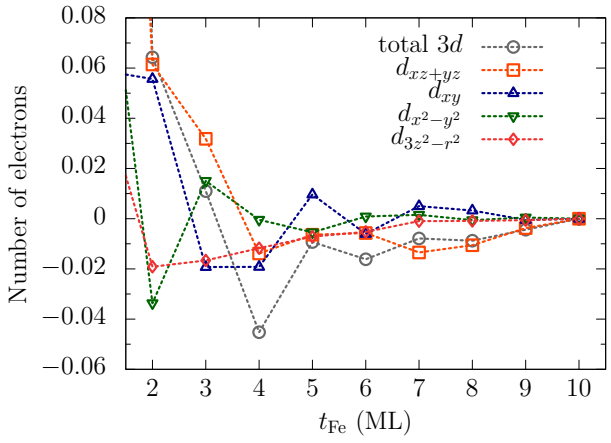

Figure 6: Thickness dependence of the number of 3d electron on the interface Fe. The relative values with respect to those of Fe 10ML are shown. The colors of grey, orange (yellow), blue, green, and red are used for total 3d orbital, d_{xz+yz}, d_{xy}, $d_{x^2-y^2}$, and $d_{3z^2-r^2}$, respectively.

3.4 Thickness dependences of interface electronic structure and number of electrons

Thickness dependence in MAE has a relationship with the number of electrons (NOE) in the 3d orbital of minority spin state on the interface Fe. In the large variation range of MAE ($<$ Fe 4ML), the NOE decreases as thickness, and in the odd-even alternating range ($\geq$ Fe 4ML) its NOE does not synchronize so much with the MAE, as shown in Fig. 6. For the former, the number of Fe

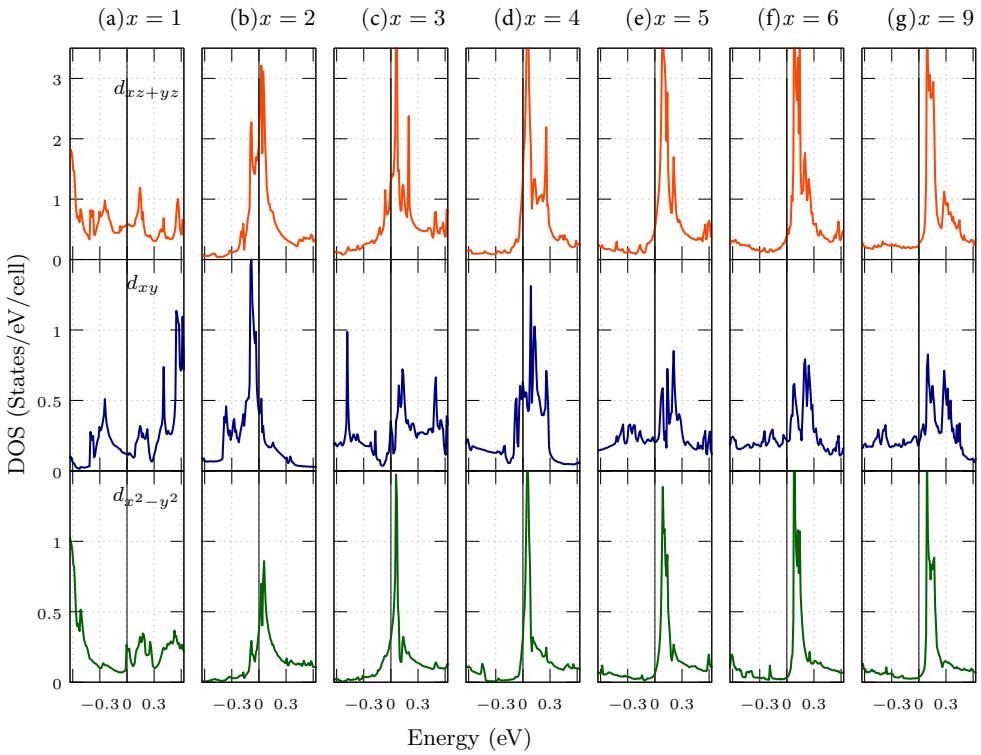

Figure 7: Projected density of states (PDOS) for the interface state in Cr/Fe(xML)/MgO; (a)–(g) for $x = 1-6$ and 9, respectively. The top, middle, bottom rows in the panels show the components of d_{xz+yz}, d_{xy}, and $d_{x^2-y^2}$.

works as hole doping, while in the latter the MAE may be influenced by the details of electronic structures at the interface. Interestingly, note that the NOEs of d_{xy} and $d_{x^2-y^2}$ show an alternating behavior in their relative values (See Fig. 6). Indeed, the alternating nature appears at the d_{xy} component in the band dispersions (not shown) and PDOS(see Fig. 7).

The number of 3d electrons at the interface Fe is summarized in Fig. 6. The total number of 3d electron decreases as the thickness increases until Fe 4ML. This decrease is in accordance with the relationship of electronegativity between Fe and Cr. The electrons on Fe of larger electronegativity gradually increases as the thickness of Fe increases from Fe 4ML.

Figure 7 shows the series of PDOS for interface states. Except for $x = 1$, the sharp peaks appear, implying the localized nature of wave functions. It is worthy to notice that the series of $x = 2-5$ do not show a simple rigid band filling. The shape of d_{xy} component changes while that of $d_{x^2-y^2}$ is kept without any large change. In details, the peaks of d_{xy} and $d_{x^2-y^2}$ are located just below and above the E_{F} level, respectively, in Fe 2ML, and as the thickness the peaks of d_{xz+yz} moves to higher energies with that of $d_{x^2-y^2}$. Additionally, it is interesting to see the PDOS peak sharpen in the thicker systems (see the case of $x = 9$). The origin of interface states energy shift is speculated as an orbital hybridization with the Cr underlayer. At the Cr/Fe interface, the 3d orbital components at E_{F} was shifted due to the hybridization to a higher energy for Cr and to a lower energy for Fe. This realizes the electron transfer from Cr to Fe atoms, showing a property of smaller electronegativity for Cr. Consequently, the 3d orbital on the Fe of Fe/MgO interface can get electrons as the thickness of Fe layer decreases. Indeed, it was observed clearly in the Fe layer with small x's as a vicinity effect of Cr. Interestingly, the similar energy lowering of IS occurs as the decrease of in-plane lattice constant [34], inducing the modulations in MAE.

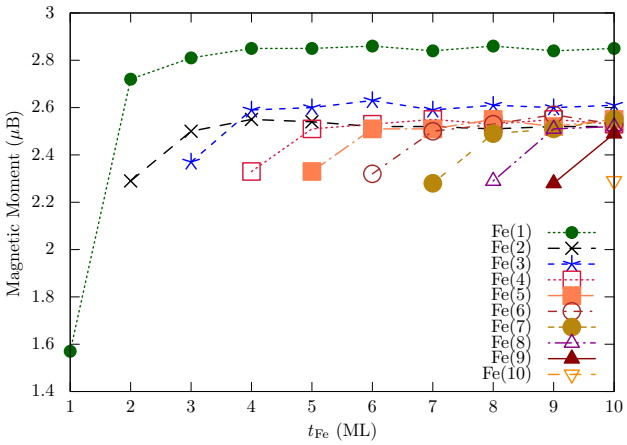

Figure 8: Atomic magnetic moment of Fe in the ferromagnet layer, Fe(1) are located at the interface of MgO.

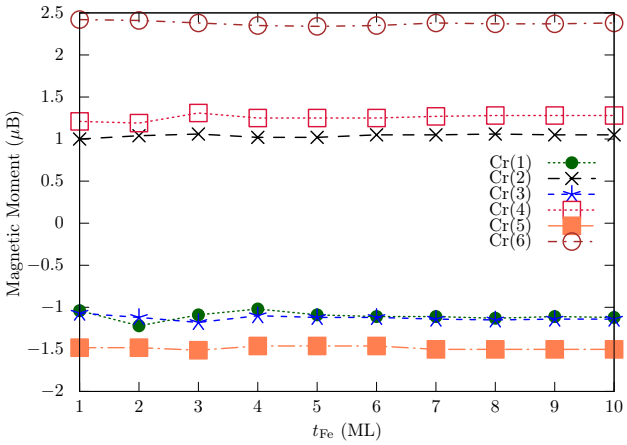

Figure 9: Atomic magnetic moment of Cr in the ferromagnet layer, Cr(1) are located at the interface with Fe.

3.5 Variation of the atomic magnetic moment

We report the results of atomic magnetic moments obtained by integrating the spin density in the atomic sphere with the radius (Cr: 0.90 Å, Fe: 0.90 Å), as shown in Fig. 8 and Fig. 9. As general trends the Fe magnetic moment is enhanced (2.8 μ_B) and reduced (2.3 μ_B) at the Fe/MgO and Cr/Fe interfaces, respectively, compared with those of the inside layers (2.5 μ_B). In the Cr layer, the magnetic moments couples also antiferromagnetically between the neighboring layers. These configurations are similar to the previous theoretical work on the Fe(001)/MgO/Cr/Fe magnetic tunnel junctions [35]. Note that the magnetic alignment related with the Cr atoms has not been known in the thin film materials (devices). To bulk Cr, an incommensurate antiferromagnetic spin-density wave has been known for a long time [36] and the interface with Fe may possibly show a noncollinear magnetic configuration [37].

As shown in Fig. 9, the magnetic moment on Cr(6) is larger than those of the other Cr MLs, because this atom faces to vacuum and the electron wave function is more localized near the vacuum. This feature contributes to larger magnetic moment.

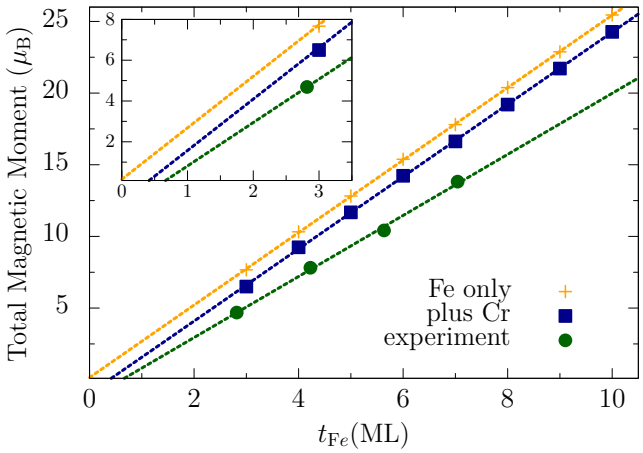

Figure 10: Thickness dependence of magnetizations, compared with the available experimental data(ref. [32]). Plus symbol indicates total magnetizations contributed from Fe atom only, solid box includes the contribution of Cr, bullet indicates experimental data.

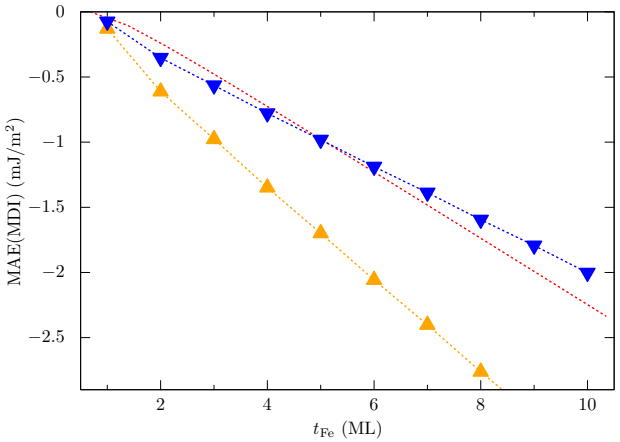

Figure 11: Theoretical MAE(MDI) (yellow triangles), normalized MAE(MDI) (blue reverse triangles), and experimental MAE(SA) (red dots), the dashed lines are only guide.

3.6 Total magnetizations

In the theoretical approach we obtained the magnetic dead layer (MDL) with 0.053 nm thick at most, while the experiment clearly showed the MDL with 0.1 nm thick [32]. The theoretical magnetization is larger than the experimental one by about 24 % at the Fe 5 ML, as shown in Fig. 10. These differences could be ascribed to an alloying effect at the Cr/Fe interface in the experiment. This allows to draw a suppression of the in-plane anisotropy from MDI contribution, or alternatively an enhancement in the strength of interface perpendicular anisotropy. The nearest neighbor pairs of Cr–Cr and Fe–Cr tend to enhance the antiferromagnetic coupling between the magnetic moments, and possibly inducing a noncollinear magnetic structures due to a competition in magnetic couplings [37]. Associated with such complexity in magnetic configuration, the MAE(SA) modulates due to the change in MDI.

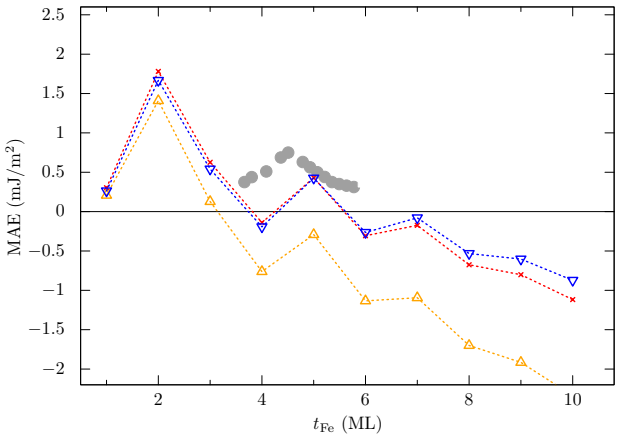

Figure 12: Total magnetic anisotropy energy (MAE), compared with the experimental data (bullets)(ref. [32]). The open yellow triangle symbol specifies the data estimated theoretically; MAE(SOI)+MAE(MDI), the reverse blue triangle symbol represents the MAE(SOI+MDI) after the 26% reduction of theoretical atomic moment, and the red cross symbol represents the sum of the theoretical MAE(SOI) and the shape anisotropy MAE(SA) estimated using the experimental magnetization.

3.7 Shape anisotropy

The shape anisotropy is realistically important for determining the whole magnetic anisotropy. When we compare our MAE(SOI) with those from measurements, the shape anisotropy needs to be estimated precisely. Here, we estimated the shape anisotropy energy, MAE(SA), in two ways; from the MDI [31] using the theoretical atomic magnetic moments and the estimation $(-\mu_0 M_s^2/2)$ using the experimental saturation magnetization (M_s) [32]. In the former, all the Cr layer were also taken into account. This shape anisotropy contribute to the in-plane component, large negative value means more reduction to the MAE(SOI). So we could observe that the calculation from pure dipole-dipole interaction [31] provide much reduction compared to the one extracted from experimental ones [32]. Just as described in Fig. 10, the estimation of total magnetization are overestimate experimental value, therefore we consider the case of normalized ones. Later we can use this value as the corrected factor of the MAE(MDI).

3.8 Total MAE

Figure 12 reports the total MAE, namely summation of MAE(SOI) and MAE(SA), in comparison with the available experimental data. This figure shows that our estimation is much reduced due to large in-plane contribution from the MDI. As shown in Fig. 11, the experimental MAE(SA) is much reduced in absolute, compared with the theoretical one. This is an origin why we have so much reduced value. By considering the reduced MDI (rMDI), we could obtain that the MAE (SOI+rMDI) describe in the blue reverse triangle. In this result we could observe an agreement with the experimental data [32].

4 Discussions

The obtained MAE(SOI) result can be compared to Bruno relation [38] in order to confirm the validness of our calculation results. This relation can describe MAE in the ferromagnetic transition metals like Fe, Co, Ni. In Fig. 13, we can observe that in even number of ferromagnet layers the

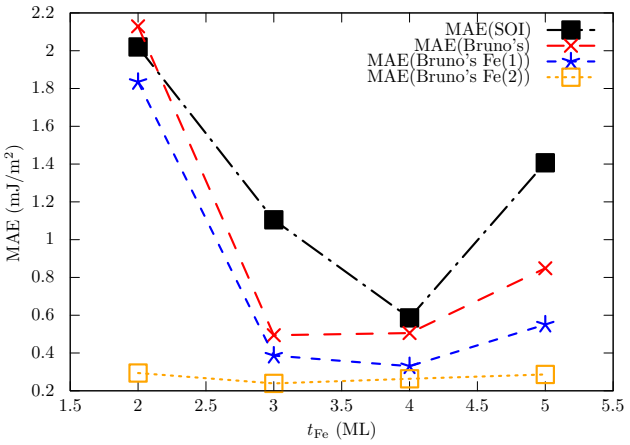

Figure 13: The estimation from Bruno's relation compared to the calculation of MAE from SOI. Black solid square represent MAE from SOI, red cross symbol are MAE calculated from Bruno relation, blue star symbol are the contribution from Fe(1) at the interface, and orange empty square symbol are contribution from Fe(2).

MAE(SOI) is close to the value estimated by assuming 62 meV to the spin-orbit coupling constant in the Bruno relation. This much underestimates the MAE for the odd number cases. This relation may not be filled for the complex system and the system with a large spin orbit coupling constant. In another way, this model is too simple for the cases of odd ML. Still, we could expect the same out-of-plane tendency for these numbers of ML in Fig. 13. We could consider that the main contribution of magnetic anisotropy energy comes from the first layer of interface iron with the MgO. The contribution of nearest neighbor is a constant around 0.2 mJ/m^2, and the contribution from next nearest neighbor is almost zero. Therefore, the latter is not included in Fig. 13.

In the case of consideration when we decrease the thickness of Fe layer, for example become 2ML, the ferromagnetic state may become unstable against thermal disturbance. This could be denied in a discussion of Cr–Fe magnetic interaction. The Fe at the Cr/Fe interface has a strong antiferromagnetic interaction of Heisenberg type. This stabilizes the ferromagnetic state of Fe thin layer. The previous works reported large exchange interactions of $J = 69$ meV and $|J|$=59, 20 meV for Fe-Fe and Cr-Fe nearest neighbors, [37, 39, 40] respectively. These values could be enough to maintain the ferromagnetic states at room temperatures. However, practically, associated with the existence of magnetic dead layer in such system, [32] Fe atom may diffuse into the Cr layer during the fabricating process at high temperatures. Indeed, when exchanging the Fe and Cr atoms at the Cr/Fe interface in Fe 4ML, the total energy does not become so higher (50 meV/in-plane Fe).

As shown in Figs. 4 and 7 the interface state discussed here is presented just as some sharp peaks in this work. The main body of states is on E_F or just above E_F by less than 0.2 eV. These energy levels are located at the same energy range in which the enhanced magnetic tunneling spectra appears [4]. The interface states in the present work may have the potential to make a state resonating with the conduction electron through the $s-d$ interaction at the interface [41]. Indeed, the enhanced spectra in the spin-dependent tunnel conductance has been observed, implying some unknown/non-resolved mechanism behind [2, 16].

The Fe layer, forming a quantum well structure, is terminated at the Fe/MgO and Cr/Fe interfaces. At the edges, the amplitudes of wave function have a feature of odd-even alternating behavior in the one dimensional model chain of which the atomic site is connected with electron transfer integral. The d_{xy} component at the Fe/MgO interface is largely affected due to its non-bonding nature, and can be sensitive to external perturbation from the other edge of Cr/Fe

interface. The electron transfer between the d_{xy} orbitals of neighboring Fe MLs is proportional to $T_{xy,xy}(\mathbf{k}) \sim e^{i\mathbf{k}\cdot\mathbf{R}}\{3t(dd\sigma)+2t(dd\pi)+4t(dd\delta)\}/9$, and is not negligible because the absolute of transfer integral can reach to about 0.1 eV [33]. Consequently, as an edge effect of the model chain, some non-negligible changes of d_{xy} are supposed to appear at the interface states.

5 Summary

We performed first principles electronic structure calculations for the interface systems with Cr underlayer of Fe/MgO interface and estimated the MAE originating from the SOI and MDI. The exotic oscillating behavior was observed in the MAE from SOI. We found that the DFT approach can describe the MAE with good accuracy, compared with the experimental data. Our calculation shows that the MAE(SOI) in 5ML system with 1.5 mJ/m^2 is comparable to the experimental ones. The series of total MAE's indicated perpendicular and in-plane magnetic anisotropies in the Cr-underlayer Fe/MgO. The reduction by the in-plane shape anisotropy energy was considered as the correction factor to the pure DFT calculation approach. By introducing the rescaled magnetization similar to the experimental one, the thickness range of perpendicular magnetic anisotropy was found to correspond to experimental result. From the electronic structure, the dispersionless and saddle point natures appearing in the band dispersions around $\mathbf{k}_1$ were found to play the important role in the perpendicular anisotropy. In the Fe 2ML, particularly, the flat bands consisting of d_{xz}, d_{yz}, d_{xy}, $d_{x^2-y^2}$ are located just below and above the Fermi level. These bands contribute to the large MAE(SOI) of 2 mJ/m^2. The change of interface states was discussed as the origin of change in the perpendicular magnetic anisotropy. The detail electronic and magnetic properties of the Cr buffered Fe/MgO slab systems might be useful in future materials design for such multi-functional interfaces.

Acknowledgement

The first-principles calculations were performed using the facilities of the Supercomputer Center, Institute for Solid State Physics, the University of Tokyo, Japan. This research partly used computational resources of the K computer and other computers of the HPCI system provided by the AICS and Information Technology Center of Nagoya University through the HPCI System Research Project (Project ID:hp160227, hp160107, hp170168). This work was partly supported by the ImPACT Program of Council for Science, Technology and Innovation (Cabinet Office, Japan Government), and by the Computational Materials Science Initiative (CMSI), Japan. The authors (N.I and I.P.) acknowledges Japanese Government (MEXT) Scholarship in the Program for the Development of Global Human Resources for Kanazawa University.

References

[1] S. Yuasa, T. Nagahama, A. Fukushima, Y. Suzuki, and K. Ando, Nat. Mater. **3**, 868 (2004).

[2] Y. Ando, T. Miyakoshi, M. Oogane, T. Miyazaki, H. Kubota, K. Ando, and S. Yuasa, Appl. Phys. Lett. **87**, 142502 (2005).

[3] W. H. Butler, X.-G. Zhang, T. C. Schulthess, and J. M. MacLaren, Phys. Rev. B **63**, 054416 (2001).

[4] J. W. Koo, H. Sukegawa, S. Kasai, Z. C. Wen, and S. Mitani, J. Phys. D: Appl. Phys. **47**, 322001 (2014).

[5] J. C. Slonczewski, J. Magn. Magn. Mater. **159**, L1 (1996).

[6] L. Berger, Phys. Rev. B **54**, 9353 (1996).

[7] S. Ikeda, K. Miura, H. Yamamoto, K. Mizunuma, H. D. Gan, M. Endo, S. Kanai, J. Hayakawa, F. Matsukura, and H. Ohno, Nat. Mater. **9** , 721 (2010).

[8] X. Liu, W. Zhang, M. J. Carter, and G. Xiao, J. Appl. Phys. **110**, 033910 (2011).

[9] S. Miwa, J. Fujimoto, P. Risius, K. Nawaoka, M. Goto, and Y. Suzuki, Phys. Rev. X **7**, 031018 (2017)

[10] C. Zhang, S. Fukami, H. Sato, F. Matsukura, and H. Ohno, Appl. Phys. Lett. **107**, 012401 (2015)

[11] T. Inokuchi, H. Yoda, Y. Kato, M. Shimizu, S. Shirotori, N. Shimomura, K. Koi, Y. Kamiguchi, H. Sugiyama, S. Oikawa, K. Ikegami, M. Ishikawa, B. Altansargai, A. Tiwari, Y. Ohsawa, Y. Saito, and A. Kurobe, Appl. Phys. Lett. **110**, 252404 (2017)

[12] Y. Shiota, T. Nozaki, F. Bonell, S. Murakami, T. Shinjo, and Y. Suzuki, Nat. Mater. **11**, 39 (2012).

[13] K. Nawaoka, S. Miwa, Y. Shiota, N. Mizuochi, and Y. Suzuki, Appl. Phys. Express **8**, 063004 (2015).

[14] V. V. Kruglyak, S. O. Demokritov, and D. Grundler, J. Phys. D: Appl. Phys. **43**, 264001 (2010).

[15] R. Shimabukuro, K. Nakamura, T. Akiyama, and T. Ito, Physica E **42**, 1014 (2010).

[16] P.-J. Zermatten, G. Gaudin, G. Maris, M. Miron, A. Schuhl, C. Tiusan, F. Greullet, and M. Hehn, Phys. Rev. B **78** 033301 (2008).

[17] I. Rungger, O. Mryasov, and S. Sanvito, Phys. Rev. B **79**, 094414 (2009).

[18] C.-G. Duan, J. P. Velev, R. F. Sabirianov, Z. Zhu, J. Chu, S. S. Jaswal, and E. Y. Tsymbal, Phys. Rev. Lett. **101**, 137201 (2008).

[19] K. Nakamura, R. Shimabukuro, Y. Fujiwara, T. Akiyama, T. Ito, and A. J. Freeman, Phys. Rev. Lett. **102**, 187201 (2009).

[20] A. Hallal, H. X. Yang, B. Dieny, and M. Chshiev, Phys. Rev. B. **88**, 184423 (2013).

[21] T. Nozaki, Y. Shiota, M. Shiraishi, T. Shinjo, and Y. Suzuki, Appl. Phys. Lett. **96**, 022506 (2010).

[22] S. S. P. Parkin, N. More, and K. P. Roche, Phys. Rev. Lett. **64**, 2304 (1990).

[23] D. F. Johnson, D. E. Jiang, and E. A. Carter, Surf. Sci. **601**, 699 (2007).

[24] T. Oda and A. Hosokawa, Phys. Rev. B **72**, 224428 (2005).

[25] K. Laasonen, A. Pasquarello, R. Car, C. Lee, and D. Vanderbilt, Phys. Rev. B **47**, 10142 (1993).

[26] J. P. Perdew, J. A. Chevary, S. H. Vosko, K. A. Jackson, M. R. Pederson, D. J. Singh, and C. Fiolhais, Phys. Rev. B **46**, 6671 (1992).

[27] N. D. Mermin, Phys. Rev. **137**, A1441 (1965).

[28] T. Oda, J. Phys. Soc. Jpn. **71**, 519 (2002).

[29] H. J. Monkhost and J. D. Pack, Phys. Rev. B **13**, 5188 (1976).

[30] M. Tsujikawa, A. Hosokawa, and T. Oda, Phys. Rev. B **77**, 054413 (2008).

[31] L. Szunyogh, B. Újfalussy, and P. Weinberger, Phys. Rev. B **51**, 9552 (1995).

[32] T. Nozaki, A. Kozioł-Rachwał, W. Skowroński, V. Zayets, Y. Shiota, S. Tamaru, H. Kubota, A. Fukushima, S. Yuasa, and Y. Suzuki, Phys. Rev. Appl. **5**, 044006 (2016).

[33] D. S. Wang, R. Wu, and A. J. Freeman, Phys. Rev. B **47**, 14932 (1993).

[34] D. Yoshikawa, M. Obata, and T. Oda, JPS Conf. Proc. **5**, 011012 (2015).

[35] J. Zhang, Y. Wang, X.-G. Zhang, and X. F. Han, Phys. Rev. B **82**, 134449 (2010).

[36] S. Cottenier, B. De Vries, J. Meersschaut, and M. Rots, J. Phys.: Condens. Matter **14**, 3275 (2002).

[37] M. Yu. Lavrentiev, R. Soulairol, Chu-Chun Fu, D. Nguyen-Manh, and S. L. Dudarev, Phys. Rev. B **84**, 144203 (2011).

[38] P. Bruno, Phys. Rev. B **39**, 865 (1989).

[39] H. Hasegawa, Phys. Rev. B **42**, 2368 (1990).

[40] M. Ogura, H. Akai, and J. Kanamori, J. Phys. Soc. Jpn. **80**, 104711 (2011).

[41] J. M. Ziman, *Principles of the theory of solids*, (Cambridge University Press, Cambridge, 1972), p. 343.